Scaffold-Mediated Static Transduction of T Cells for CAR-T Cell Therapy

*Pritha Agarwalla, Edikan A. Ogunnaike, Sarah Ahn, Frances S. Ligler, Gianpietro Dotti, and Yevgeny Brudno**

Chimeric antigen receptor T (CAR-T) cell therapy has produced impressive clinical responses in patients with B-cell malignancies. Critical to the success of CAR-T cell therapies is the achievement of robust gene transfer into T cells mediated by viral vectors such as gamma-retroviral vectors. However, current methodologies of retroviral gene transfer rely on spinoculation and the use of retronectin, which may limit the implementation of cost-effective CAR-T cell therapies. Herein, a low-cost, tunable, macroporous, alginate scaffold that transduces T cells with retroviral vectors under static condition is described. CAR-T cells produced by macroporous scaffold-mediated viral transduction exhibit >60% CAR expression, retain effector phenotype, expand to clinically relevant cell numbers, and eradicate CD19$^+$ lymphoma in vivo. Efficient transduction is dependent on scaffold macroporosity. Taken together, the data show that macroporous alginate scaffolds serve as an attractive alternative to current transduction protocols and have high potential for clinical translation to genetically modify T cells for adoptive cellular therapy.

Adoptive T cellular therapy harnesses and redirects a patient's own immune system and has emerged as a promising personalized treatment modality to treat cancer [1–3] and various other diseases.[4,5] The most successful example has been the adoptive transfer of chimeric antigen receptor redirected T cells (CAR-T cells) targeting the CD19 expressed by B-cell malginancies, that received FDA approvals in 2017.[6,7] With the compelling success of CD19-specific CAR T-cell therapies, efforts are now being directed toward broadening the application of CAR-T cells to other cancer types.[8–11] One of the key steps involved in CAR T- cell therapy is the genetic modification of T cells ex vivo, which endows T cells with stable expression of the CAR molecule that redirect T-cell specificity towards tumor antigens. However, inexpensive strategies to generate large numbers of genetically modified functional T cells remains a central challenge to the widespread use of CAR-T cells. Thus, development of culture platforms enabling ex vivo genetic engineering of T cells followed by expansion to clinically relevant cell numbers is of immense importance for the success of CAR-T cell therapy.

A number of different approaches are being explored to genetically engineer T cells ex vivo. [12–17] Among them, lentiviral or retroviral vector-based gene transfer represents the most successful approach.[16] When retrovirus is used to generate CAR-T cells, T cells isolated from patients are first stimulated with agonistic anti-CD3 and anti-CD28 antibodies and then incubated with retrovirus because quiescent T cells are refractory to retrovirus-mediated insertion.[18,19] Because of the short distance the retrovirus can travel in solution by Brownian motion (less than 600 µm within one half-life),[20,21] activated T cells and retrovirus must be brought into contact either by spinoculation in the presence of transduction-promoting agents such as retronectin or polybrene or by using microfluidic based transduction devices.[22–24] Transduction-promoting agents like polybrene[25] and protamine sulfate[26,27] as well as microfluidic transduction devices have been used with modest success,[28] while recombinant fibronectin fragment CH296 (Retronectin) represents the most widely clinically used transduction-promoting reagent for retrovirus.[29] Retronectin binds retrovirus through its heparin-binding domain and T cells via CS-1/RGD domains, bringing cells and retrovirus together and facilitating gene transfer.[30] Retronectin must be pre-coated onto a solid surface, such as polystyrene plate, flask or bag for effective co-localization of retrovirus and T cells.[30,31] Even then, gene transfer and subsequent CAR expression remain suboptimal under passive/static conditions.[32] To achieve high gene expression, retrovirus is seeded on retronectin-coated surfaces and centrifuged at high speed.[32–34] Furthermore, retronectin is a recombinant protein, and it is inherently bioreactive which can influence cell differentiation and proliferation.[35,36] Thus the development of more efficient culture systems enabling a single

Dr. P. Agarwalla, Prof. F. S. Ligler, Prof. Y. Brudno
Joint Department of Biomedical Engineering, University of North Carolina - Chapel Hill and North Carolina State University - Raleigh
1840 Enterpreneur Way, Raleigh, NC 27695, USA
E-mail: ybrudno@ncsu.edu
Dr. E. A. Ogunnaike, Dr. S. Ahn, Prof. G. Dotti
Department of Microbiology and Immunology
University of North Carolina at Chapel Hill
Chapel Hill NC 27599, USA
Prof. G. Dotti, Prof. Y. Brudno
Lineberger Comprehensive Cancer Center
University of North Carolina
Chapel Hill. 450 West Dr., Chapel Hill, NC 27599, USA

The ORCID identification number(s) for the author(s) of this article can be found under https://doi.org/10.1002/adhm.202000275

DOI: 10.1002/adhm.202000275

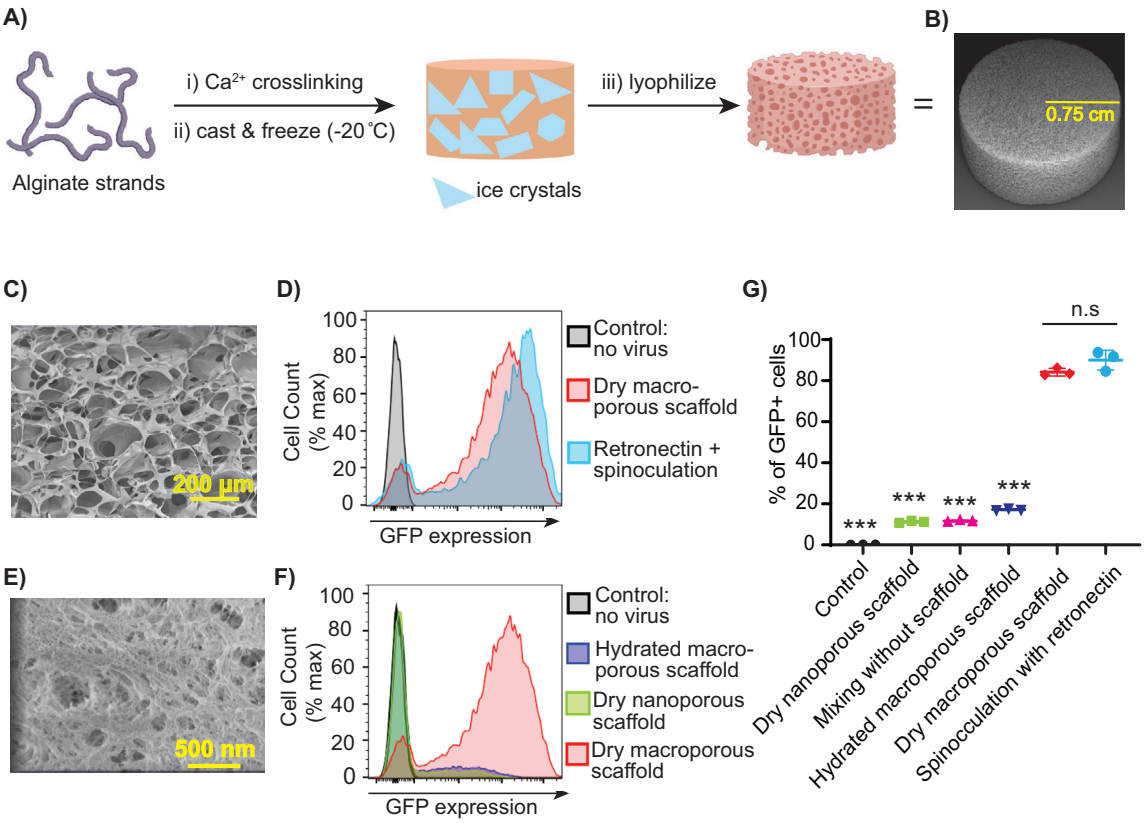

Figure 1. Dry macroporous scaffolds mediate retroviral transduction of human activated T cells. A) Schematic showing the preparation of macroporous alginate scaffolds. B,C) SEM images of dry macroporous scaffolds. D) GFP expression in activated T cells transduced with equal amounts of retrovirus seeded on dry macroporous scaffolds (red) and retronectin-coated plates with spinoculation (blue). Non-transduced control cells are represented in black. E) SEM image of dry nanoporous scaffold. F) GFP expression in T cells transduced with retrovirus seeded on dry macroporous scaffolds (red), hydrated macroporous scaffolds (purple), and dry nanoporous scaffolds (green). Control non-transduced cells are in black. G) Quantification of GFP^+ cells (***$p < 0.0001$ with respect to dry macroporous scaffolds, Student's *t*-test)

step ex vivo engineering process of T cells under static conditions without retronectin or spinoculation would significantly reduce the cost of CAR-T cell manufacturing when retrovirus is used as gene delivery system.

We have developed a 3D macroporous scaffold as an efficient, single-step, static platform to engineer T cells with viral vectors. We hypothesized that 3D dimensional scaffolds with macroporosity and high capacity to absorb water [37] would allow colocalization of retrovirus and T cells as achieved by using retronectin. We prepared macroporous scaffolds from calcium-crosslinked alginate, which is a GMP-compliant and FDA-approved biomaterial extensively used for many biomedical applications due to its biocompatibility, low toxicity, low cost, and mild gelation by divalent cations.[38] We observed that dry, hygroscopic, and macroporous alginate scaffolds facilitate the interaction of retrovirus and T cells and enables efficient gene transfer in a single step without spinoculation and without affecting functionality and viability of engineered T cells. Thus, these scaffolds represent a simple, cost-effective and tunable platform technology for generating highly functional T cells for adoptive cellular therapy.

The macroporous alginate scaffolds were prepared by mild cryogelation (**Figure 1**A). Imaging by scanning electron microscopy (SEM) revealed well connected, 100–200 µm pores throughout the scaffold (Figure 1B,C). Alginate scaffolds were tested for human T cell transduction using gamma retrovirus. T cells obtained from the peripheral blood (PBMCs) of the three different health donors were activated with agonistic anti-CD3 and anti-CD28 antibodies. Activated T cells were then seeded on either conventional spinoculated retrovirus- and retronectin-coated plates or retrovirus seeded into the alginate scaffolds. A preliminary screen of transduction efficiency at multiplicities of infection (MOIs) of 1, 2, and 4 (Figure S1, Supporting Information) using retrovirus encoding GFP demonstrated efficient transduction and an MOI of 2 was chosen for further experiments. As shown in Figure 1D, 72 h after incubation with equal amounts of retrovirus (MOI 2), T cells expressing GFP on the scaffolds were comparable to those transduced by retronectin coated plates with spinoculation (85 ± 3% versus 90 ± 5% GFP^+ cells). For reasons not completely understood, these results showed improved transduction in both groups as compared to viral transduction in the preliminary experiments (Figure S1, Supporting Information, 49% versus 73.5%, respectively). Despite this, very little variability was noted across three different PBMC donors (Figure 1D).

To evaluate whether the macroporosity of the scaffolds affects the interaction between retrovirus and T cells, we fabricated nanoporous scaffolds (Figure 1E), which can absorb retrovirus

and T cells, but lack the macroporosity that permits T cell entry into the scaffold. To test whether the sponge-like effect was also needed to create proximity between retrovirus and T cells, we tested hydrated macroporous scaffolds, which have the large pores, but lack the active flow of fluid into the internal pores. We found that neither the dry nanoporous scaffold, nor the hydrated macroporous gel allowed efficient gene transfer as compared to dry macroporous scaffold (Figure 1F,G). In the hydrated macroporous scaffold, only ≈12% of cells expressed GFP, indicating that absorption of virus and T cells on the scaffold permit physical contact between retrovirus and T cells, but not nearly as efficiently as the colocalization in the pores accomplished using the dry macroporous alginate scaffold. Future work will explore the use of a chemical kinetics model to further understand the effect of pore size on transduction efficiency of above described alginate scaffolds.

Next, we assessed whether the CAR-T cells generated using the dry macroporous scaffold were functional in vitro. For these experiments we used retrovirus encoding a CAR specific for the CD19 antigen (CD19.CAR). Activated T cells obtained from three healthy donors were seeded on alginate scaffolds or retronectin-coated plates loaded with CD19.CAR retrovirus. Upon removal from the scaffold or retronectin, T cells were maintained in culture, and CAR expression was analyzed on day 3 and day 9 after transduction. As shown in **Figure 2**A, both scaffold and retronectin promoted comparable transduction efficiency, and CAR expression remained unaltered upon expansion through day 9 (Figure 2A; Figure S2, Supporting Information). CAR-T cells were also analyzed for immune composition by flow cytometry. CAR-T cells generated by conventional means or scaffold showed no differences for expression of CD4, CD8, memory (CD45RA, CCR7) or exhaustion (PD-1, Lag3) markers (Figure 2C; Figures S3 and S4, Supporting Information). Next, to evaluate anti-tumor effects in vitro, control non-transduced T cells (NT-cells) and CD19.CAR-T cells generated either by scaffold-mediated or retronectin-mediated transduction were co-cultured with CD19 positive target cells (Daudi) and CD19 negative target cells (U937 CHLA-A2+). Since effector-to-target ratio is a strong determinant of cytolytic activity, we measured cytotoxicity at two different effector-to-target ratios (1:2 and 1:5) based on previous literature.[39] NT cells did not eliminate either of the tumor cells, while both CD19.CAR-T cells transduced using either the scaffold or retronectin/spinoculation eliminated $CD19^+$ Daudi cells (Figure 2E; Figure S5, Supporting Information), but not $CD19^-$ U937 cells (Figure S6, Supporting Information), indicating preserved antigen specificity of redirected T cells. From the same co-culture experiments, cytokines were measured in supernatant collected after 24 h incubation, and CD19.CAR-T cells released IL-2 and interferon IFN-γ in response to Daudi cells (Figures 2F,G). Finally, CD19.CAR-T cells generated using both the scaffold and retronectin methods showed comparable proliferative capacity in response to Daudi cells (Figure 2B). Taken together, these results demonstrate that the alginate scaffold generates highly functional CAR-T cells.

The antitumor activity of CAR-T cells observed in vitro results was confirmed in an in vivo tumor model. Daudi cells labeled with firefly luciferase (FFLuc) were intravenously (i.v.) injected in nonobese diabetic severe combined immunodeficiency NSG mice, and four days later mice ($n = 5$) were infused i.v. with either control non-transduced (NT) cells or CD19.CAR-T cells generated by either scaffold- or retronectin-mediated transduction. CD19.CAR-T cells generated by either method controlled tumor cell growth as assessed by the measurement of tumor bioluminescence intensity (**Figure 3**B,C; Figure S7, Supporting Information). Control of the tumor was associated with an improved overall survival rate (Figure 3E) and without significant toxicity as assessed by changes in body weight (Figure 3D). Thus, scaffold generated CAR-T cells were as equally functional in vivo as CAR-T cells generated by the conventional transduction with retronectin and spinoculation. Future studies will explore the promise of scaffold-mediated transduction of T cells to treat solid tumors.

In conclusion, we demonstrate that a biocompatible, macroporous alginate scaffold is as effective in generating T cells engineered with retrovirus as the commercially available retronectin owing to its macroporosity and hygroscopic nature. The dry scaffold we have developed eliminates the need for spinoculation of plates coated with retronectin and seeded with the retroviral particles, thereby simplifying the manufacturing process. CAR-T cells generated through static transduction on the macroporous alginate gel fully maintained their functionality. These data support the potential for the use of an easily synthesizable and low-cost transduction platform to enable generation of highly functional T cells for adoptive cell therapy. This simple platform is also likely to address the need for efficient transduction methods useful with other refractory cell types.

Experimental Section

Preparation of Macroporous Alginate Scaffold: Macroporous alginate scaffold was prepared by a procedure reported previously.[40] A 2% solution ultrapure alginate (Pronova, MVG) in water was vigorously stirred with 4% calcium gluconate for 15 min. The resulting mixture (final calcium concentration 0.01 M) was then cast in 24 well plates (1 mL per well), frozen at −20 °C overnight, and lyophilized. The scaffold was either used immediately or stored at 4 °C before use in in vitro or in vivo experiments.

Preparation of Dry Nanoporous Alginate Scaffold: Calcium crosslinked alginate gel was cast in 24 well plates and allowed to gel overnight. The gels were then subjected to multistep solvent exchange with increasing concentrations of ethanol (10, 30, 50, 70, 90, and 100% v/v), followed by drying with supercritical CO_2.[41]

Scanning Electron Microscopy: Dry macroporous scaffold was cut with a sharp razor, coated with 70 nm AuPd (Au: 60%, Pd: 40%) for 10 min at 7 nm min^{-1} and analyzed on Hitachi S-3200N Variable pressure SEM. The surface morphology of the nanoporous scaffolds was analyzed by field emission scanning electron microscopy, FESEM (Verios FE1)

Cell Lines and Retronectin-Mediated CAR-T Cell Generation: Daudi cells expressing firefly luciferase were maintained in RPMI 1640 (Gibco) supplemented with 10% fetal bovine serum (Gibco), 2 mmol L^{-1} GlutaMax (Gibco), penicillin (100 units mL^{-1}) and streptomycin (100 mg mL^{-1}; Gibco). All cells were maintained at 37 °C with 5% CO_2. Peripheral blood mononuclear cells were isolated from buffy coats (Gulf Coast Regional Blood Center) using Lymphoprep medium (Accurate Chemical and Scientific Corporation) and activated on plates coated with 1 mg mL^{-1} CD3 (Miltenyi Biotec) and CD28 (BD Biosciences) monoclonal antibodies. GFP.encoded or CD19.CAR encoded retrovirus was prepared according to method reported previously.[39] The viral titer was measured by standard flow cytometry assay.[42] Serially diluted viral stocks were added to HEK293T cells. 72 h later, GFP expression was analyzed by flow cytometry. Population with 5–20% GFP+ cells were used to calculate the viral titer (transducing units per mL) using the following equation: Titer (TU mL^{-1}) = (initial cell count * %GFP+)/(volume of virus * dilution factor).

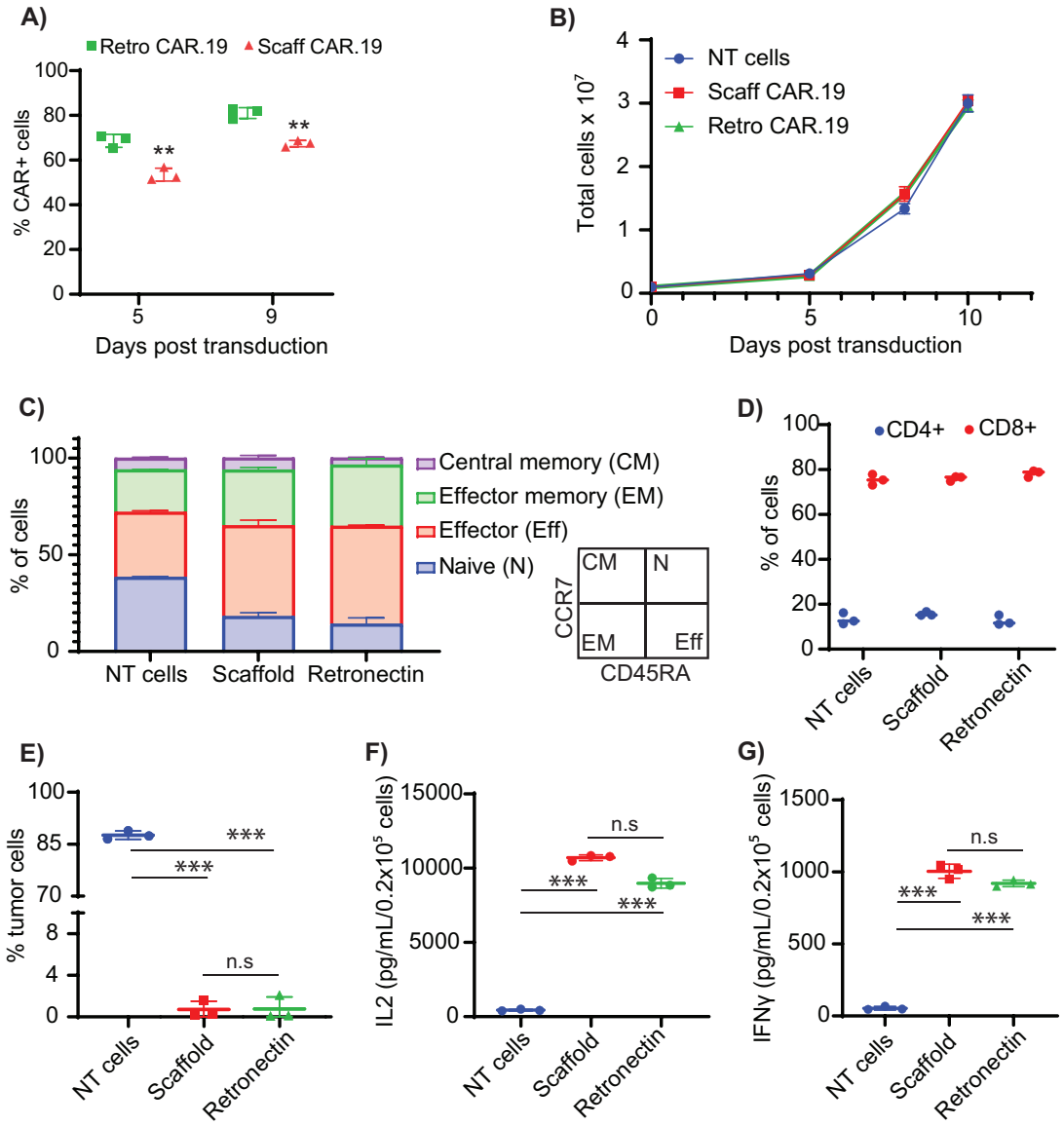

Figure 2. Scaffold-generated CD19.CAR-T cells show similar functional activity to retronectin/spinoculation-derived CAR-T cells in vitro. A) CD19.CAR expression in T cells transduced on retronectin-coated plates or on macroporous scaffolds in comparison to non-transduced control T cells (NT cells). B) Ex vivo expansion of T cells transduced on retronectin-coated plates or on macroporous scaffolds or NT cells. C, D) Immunophenotypic composition of CAR-T cells obtained via scaffold-mediated or retronectin/spinoculation-mediated transduction and NT cells at day 12 of culture. Analysis was performed gating on CAR-expressing T cells except for NT cells. E) Percentage of $CD19^+$ Daudi cells remaining (tumor cells) when co-cultured with scaffold-generated, retronectin/spinoculation-generated CAR-T cells or control NT cells. Tumor cells and T cells were plated at 1:5 effector to target ratio. T cells and tumor cells were quantified by flow cytometry on day 5 of co-culture. ***$p < 0.0001$ unpaired Student's t-test. F) IFN-γ and IL-2 release into co-culture supernatant by scaffold-generated, retronectin/spinoculation-generated CAR-T cells, and control NT cells after 24 h of coculture with tumor cells as assessed by ELISA. ***$p < 0.0001$; two-way ANOVA with Tukey correction. Data are represented as the mean ± SD from three experiments, each derived from a different PBMC donor.

MOI was calculated as the ratio of the number of transducing viral particles used to the actual number of cells. Activated T cells (1×10^6 cells) were transduced with GFP.encoded or CD19.CAR encoded retroviral supernatants[39] (2 mL viral supernatant with $\approx 1 \times 10^6$ TU mL^{-1}, MOI: 2) on retronectin-coated 24-well plates (Takara Bio Inc.). Two days after transduction, transduced T cells were expanded in 50% Click's Medium (Irvine Scientific) and 50% RPMI-1640 supplemented with 10% HyClone fetal bovine serum (GE Healthcare), 2 mmol L^{-1} GlutaMax (Gibco). penicillin (100 nits mL^{-1}), and streptomycin (100 mg mL^{-1}; Gibco) with 10 ng mL^{-1} IL7 and 5 ng mL^{-1} of IL15 (PeproTech) for 10 to 14 days before being used for functional assays

Scaffold-Mediated Generation of CAR-T Cells: Retroviral supernatant containing GFP-encoded or human CD19.CAR-encoded gamma retrovirus[39] was concentrated tenfold by Amicon centrifugation (MWCO 100 kDa, Milipore) at 4 °C, 2500 g, 15–20 min. Dry alginate scaffolds were transferred to non-tissue culture coated 24 well plates (Falcon). Concentrated retrovirus (2 mL of viral supernatant concentrated to 200 µL) and 1×10^6 activated T cells (isolated from Buffy coats and

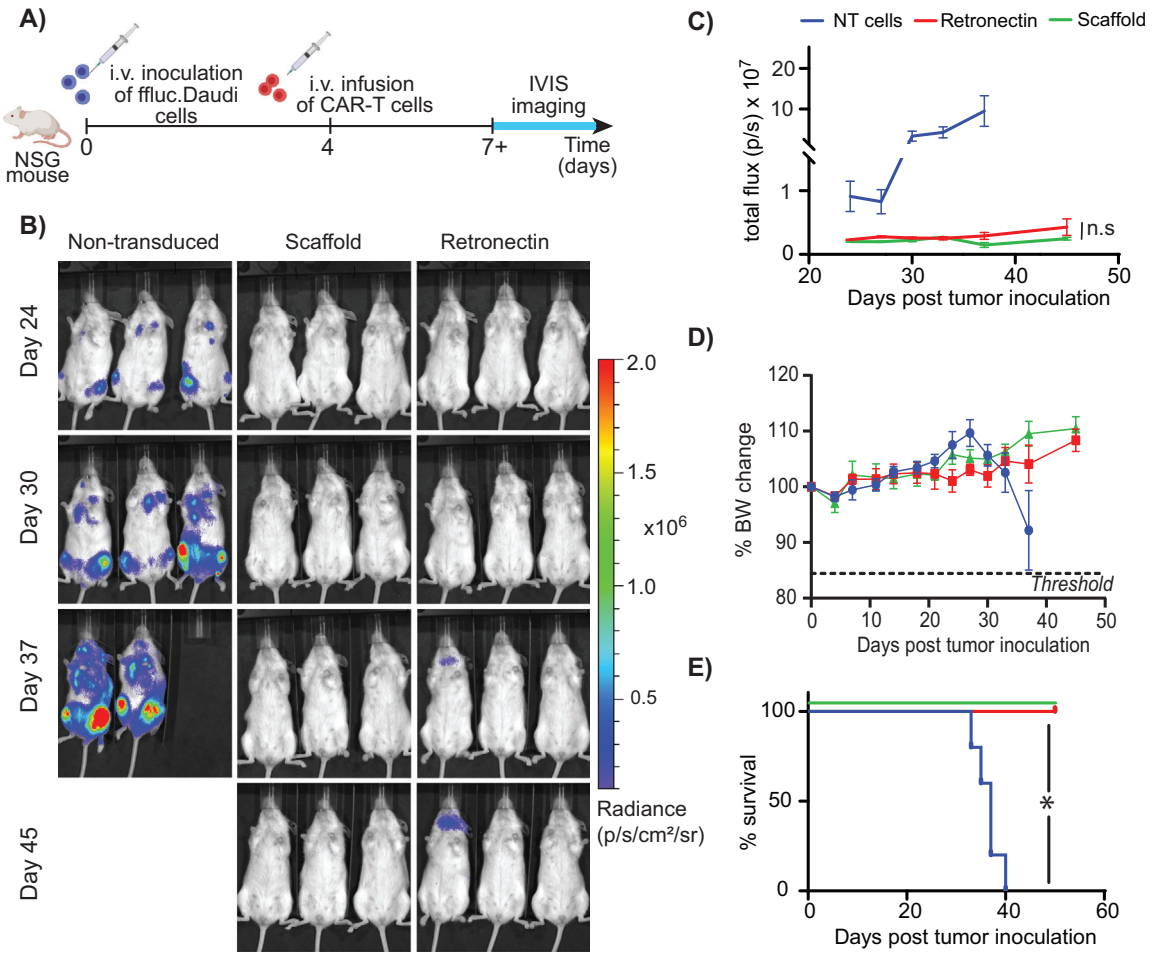

Figure 3. Scaffold-generated CD19.CAR-T cells eradicate tumors in a mouse xenograft model of lymphoma A) Experimental timeline of the lymphoma xenograft model in NSG mice using the FFLuc-labeled CD19$^+$ human Daudi tumor cells. B) Representative tumor bioluminescent images (BLI) of NSG mice inoculated with Daudi cells and treated with control NT cells or treated with CD.19.CAR-T cells generated by scaffold-mediated transduction or retronectin/spinoculation-assisted transduction. C) Kinetics of tumor growth measured by quantification of BLI. $^{**}p < 0.01$ when scaffold or CAR-T cells were compared to control NT cells, one way ANOVA. D) Body weight change and E) Survival of tumor-bearing mice treated with control NT cells or CD19.CAR-T cells generated by scaffold-mediated or retronectin spinoculation assisted transduction. $^{*}p < 0.05$, log-rank test.

activated on CD3/CD28 coated plates) in a total volume of 300 µL media were pipetted onto each scaffold (MOI: 2, same viral amount as for retronectin (above)). Control scaffolds were seeded with 1×10^6 activated T cells suspended in cell culture medium. The seeded scaffolds were incubated without any additional medium in a 5% CO_2 incubator at 37 °C for 1 h, after which 1 mL of complete medium was added. After 3 days of culture, cells were isolated from scaffolds by digesting with 1 mL 0.125 M EDTA (calcium chelator), washed twice with PBS and analyzed for GFP expression or CD19.CAR expression by flow cytometry. More than 95% of cells were recovered and viable.

Flow Cytometry and Antibodies: Monoclonal antibodies specific for human CD3 (APC-Cy7, 557 832), CD4 (APC-Cy7, 561 839), CD8 (PerCP-Cy5.5, 565 310), CD20 (FITC, 555 622), CD45RA (PE, 555 489), CD62L (BV421, 563 861), LAG3 (PE, 565 617), PD-1 (FITC, 561 035), and TIM3 (BV421, 565 563) were purchased from BD Biosciences, and CCR7 (FITC, FAB197F-100) from R&D Systems. An anti idiotype scFv monoclonal antibody was used to detect the expression of the CD19.CAR as previously described.[39] All samples were analyzed using a BD LSRII, and a minimum of 10000 events were acquired per sample. Results were analyzed using FlowJo 9 (FlowJo LLC).

Cytokine Production by CAR-T Cells: CAR-T cells were cocultured with Daudi tumor cells at 1:5 effector to target [E:T] ratio for 24 h and the culture supernatant was collected. IL-2 and IFN-γ were quantified by ELISA using the manufacturer's protocol (R&D Systems).

In Vitro Cytotoxicity: Tumor cells (Daudi) were seeded at 1×10^5 cells per well in 24-well plates. CAR-T cells normalized for transduction efficiency were added at 1:5 and 1:2 Effector:Target (E:T) ratio. On day 5 of coculture, cells were collected, and the frequency of T cells and residual tumor (CD20$^+$) cells were measured by flow cytometry.

In Vivo Antitumor Activity: Eight-to-ten weeks old female, non-obese diabetic severe combined immunodeficiency NSG (NOD.Cg-*Prkdc*^{scid} *Il2rg*^{tm1Wjl}/Sz*J*) mice were infused with 1×10^6 FFLuc-expressing Daudi cells intravenously. Four days after infusion, each mouse was intravenously injected with either 4×10^6 CD19.CAR-T cells or non-transduced (NT) cells. Tumor burden was monitored using the Xenogen-IVIS Imaging System. Mice were monitored for signs of discomfort and euthanized upon losing more than 15% of initial body weight or the development of hind-limb paresis. All procedures involving animals were done in compliance with the University's Institutional Animal Care and Use Committee.

Statistical Analysis: All statistical analysis was done using two-tailed Student's *t*-test, one way ANOVA or two-way ANOVA with Tukey post hoc

analysis using graph pad prism and noted in figures as * = $p < 0.05$, ** = $p < 0.01$, *** = $p < 0.001$.

Supporting Information

Supporting Information is available from the Wiley Online Library or from the author.

Acknowledgements

This work was supported by the North Carolina Biotechnology Center Flash Grant 2019-FLG-3812, by the National Center for Advancing Translational Sciences (NCATS), by the National Institutes of Health through Grant Award Numbers UL1TR002489, R01 CA193140, R21-CA229938-01A1, T32CA196589 and R25NS094093 and by Start-Up funds provided by the University of North Carolina at Chapel Hill and North Carolina State University at Raleigh. The authors thank the North Carolina State University College of Veterinary Medicine staff for proper care of animals used in experiments and valuable resources on training. The authors also thank the North Carolina State University flow cytometry core for training and guidance on flow cytometry analysis. SEM images were provided by James Weaver at the Wyss Institute for Biologically Inspired Engineering at Harvard as well as the Analytical Instrumentation Facility (AIF) at North Carolina State University, which is supported by the State of North Carolina and the National Science Foundation (ECCS-1542015). The AIF is a member of the North Carolina Research Triangle Nanotechnology Network (RTNN), a site in the National Nanotechnology Coordinated Infrastructure (NNCI). The authors are grateful to Hongwei Du for technical advice and assistance with data analysis.

Conflict of Interest

The authors declare no conflict of interest.

Keywords

alginate scaffold, CAR-T cells, cell therapy, immunotherapy, viral transduction

Received: February 18, 2020
Revised: May 8, 2020
Published online: June 11, 2020

[1] S. A. Rosenberg, N. P. Restifo, *Science* **2015**, *348*, 62.
[2] C. H. June, S. R. Riddell, T. N. Schumacher, *Sci. Transl. Med.* **2015**, *7*, 280ps7.
[3] A. D. Fesnak, C. H. June, B. L. Levine, *Nat. Rev. Cancer* **2016**, *16*, 566.
[4] S. Patel, R. B. Jones, D. F. Nixon, C. M. Bollard, *Cytotherapy* **2016**, *18*, 931.
[5] S. Seo, C. Smith, C. Fraser, R. Patheja, S. P. Shah, S. Rehan, P. Crooks, M. A. Neller, R. Khanna, *Blood Advances* **2019**, *3*, 1774.
[6] V. Prasad, *Nat. Rev. Clin. Oncol.* **2018**, *15*, 11.
[7] P. Sharma, G. T. King, S. S. Shinde, E. Purev, A. Jimeno, *Drugs of Today* **2018**, *54*, 187.
[8] A. I. Salter, M. J. Pont, S. R. Riddell, *Blood* **2018**, *131*, 2621.
[9] K. Watanabe, S. Kuramitsu, A. D. Posey Jr., C. H. June, *Frontiers in Immunology* **2018**, *9*, 2486.
[10] K. Newick, S. O'Brien, E. Moon, S. M. Albelda, *Annu. Rev. Med.* **2017**, *68*, 139.
[11] E. I. Lichtman, G. Dotti, *Translational Research* **2017**, *187*, 59.
[12] Y. Nakazawa, L. E. Huye, G. Dotti, A. E. Foster, J. F. Vera, P. R. Manuri, C. H. June, C. M. Rooney, M. H. Wilson, *J. Immunother.* **2009**, *32*, 826.
[13] Y. Nakazawa, S. Saha, D. L. Galvan, L. Huye, L. Rollins, C. M. Rooney, M. H. Wilson, *J. Immunother.* **2013**, *36*, 3.
[14] S. N. Maiti, H. Huls, H. Singh, M. Dawson, M. Figliola, S. Olivares, P. Rao, Y. J. Zhao, A. Multani, G. Yang, L. Zhang, D. Crossland, S. Ang, H. Torikai, B. Rabinovich, D. A. Lee, P. Kebriaei, P. Hackett, R. E. Champlin, L. J. N. Cooper, *J. Immunother.* **2013**, *36*, 112.
[15] S. Ramanayake, I. Bilmon, D. Bishop, M.-C. Dubosq, E. Blyth, L. Clancy, D. Gottlieb, K. Micklethwaite, *Cytotherapy* **2015**, *17*, 1251.
[16] R. A. Morgan, B. Boyerinas, *Biomedicines* 9, **2016**, *4*.
[17] Y. Zhao, E. Moon, C. Carpenito, C. M. Paulos, X. Liu, A. L. Brennan, A. Chew, R. G. Carroll, J. Scholler, B. L. Levine, S. M. Albelda, C. H. June, *Cancer Res.* **2010**, *70*, 9053.
[18] E. Verhoeyen, C. Costa, F.-L. Cosset, *Genetic Modification of Hematopoietic Stem Cells* **2009**, 97.
[19] Y. D. Korin, J. A. Zack, *J. Virol.* **1998**, *72*, 3161.
[20] M. Havenga, P. Hoogerbrugge, D. Valerio, H. H. van Es, *Stem Cells* **1997**, *15*, 162.
[21] S. T. Andreadis, B. O. Palsson, *Journal of Theoretical Biology* **1996**, *182*, 1.
[22] N. Moore, J. R. Chevillet, L. J. Healey, C. McBrine, D. Doty, J. Santos, B. Teece, J. Truslow, V. Mott, P. Hsi, V. Tandon, J. T. Borenstein, J. Balestrini, K. Kotz, *Sci. Rep.* **2019**, *9*, 15101.
[23] R. Tran, D. R. Myers, G. Denning, J. E. Shields, A. M. Lytle, H. Alrowais, Y. Qiu, Y. Sakurai, W. C. Li, O. Brand, J. M. Le Doux, H. T. Spencer, C. B. Doering, W. A. Lam, *Mol. Ther.* **2017**, *25*, 2372.
[24] R. Tran, D. R. Myers, J. E. Shields, B. Ahn, Y. Qiu, C. Hansen, Y. Sakurai, R. Moot, H. T. Spencer, C. B. Doering, W. A. Lam, *Blood* **2015**, *126*, 4415.
[25] L. L. Parker, M. T. Do, J. A. Westwood, J. R. Wunderlich, M. E. Dudley, S. A. Rosenberg, P. Hwu, *Hum. Gene Ther.* **2000**, *11*, 2377.
[26] E. Robinet, J. M. Certoux, C. Ferrand, P. Maples, A. Hardwick, J. Y. Cahn, C. W. Reynolds, W. Jacob, P. Hervé, P. Tiberghien, *Journal of Hematotherapy* **1998**, *7*, 205.
[27] Q. Ma, M. Safar, E. Holmes, Y. Wang, A. L. Boynton, R. P. Junghans, *The Prostate* **2004**, *61*, 12.
[28] P. Lin, D. Correa, Y. Lin, A. I. Caplan, *PLoS One* **2011**, *6*, e23891.
[29] C. H. J. Lamers, P. van Elzakker, S. C. L. van Steenbergen, S. Sleijfer, R. Debets, J. W. Gratama, *Cytotherapy* **2008**, *10*, 406.
[30] H. Hanenberg, X. L. Xiao, D. Dilloo, K. Hashino, I. Kato, D. A. Williams, *Nat. Med.* **1996**, *2*, 876.
[31] K. E. Pollok, H. Hanenberg, T. W. Noblitt, W. L. Schroeder, I. Kato, D. Emanuel, D. A. Williams, *J. Virol.* **1998**, *72*, 4882.
[32] A. Tonks, A. J. Tonks, L. Pearn, Z. Mohamad, A. K. Burnett, R. L. Darley, *Biotechnol. Prog.* **2005**, *21*, 953.
[33] P. Zhou, J. Lee, P. Moore, K. M. Brasky, *Hum. Gene Ther.* **2001**, *12*, 1843.
[34] A. Quintas-Cardama, R. K. Yeh, D. Hollyman, J. Stefanski, C. Taylor, Y. Nikhamin, G. Imperato, M. Sadelain, I. Riviere, R. J. Brentjens, *Hum. Gene Ther.* **2007**, *18*, 1253.
[35] A. J. García, M. D. Vega, D. Boettiger, *Mol. Biol. Cell* **1999**, *10*, 785.
[36] M. A. Lan, C. A. Gersbach, K. E. Michael, B. G. Keselowsky, A. J. García, *Biomaterials* **2005**, *26*, 4523.
[37] Y. Qin, *J. Appl. Polym. Sci.* **2004**, *91*, 1641.
[38] K. Y. Lee, D. J. Mooney, *Prog. Polym. Sci.* **2012**, *37*, 106.
[39] I. Diaconu, B. Ballard, M. Zhang, Y. Chen, J. West, G. Dotti, B. Savoldo, *Mol. Ther.* **2017**, *25*, 580.
[40] L. Shapiro, S. Cohen, *Biomaterials* **1997**, *18*, 583.
[41] L. Baldino, S. Concilio, S. Cardea, E. Reverchon, *Polymers* **2016**, *8*, 106.
[42] L. Sastry, T. Johnson, M. J. Hobson, B. Smucker, K. Cornetta, *Gene Ther.* **2002**, *9*, 1155.